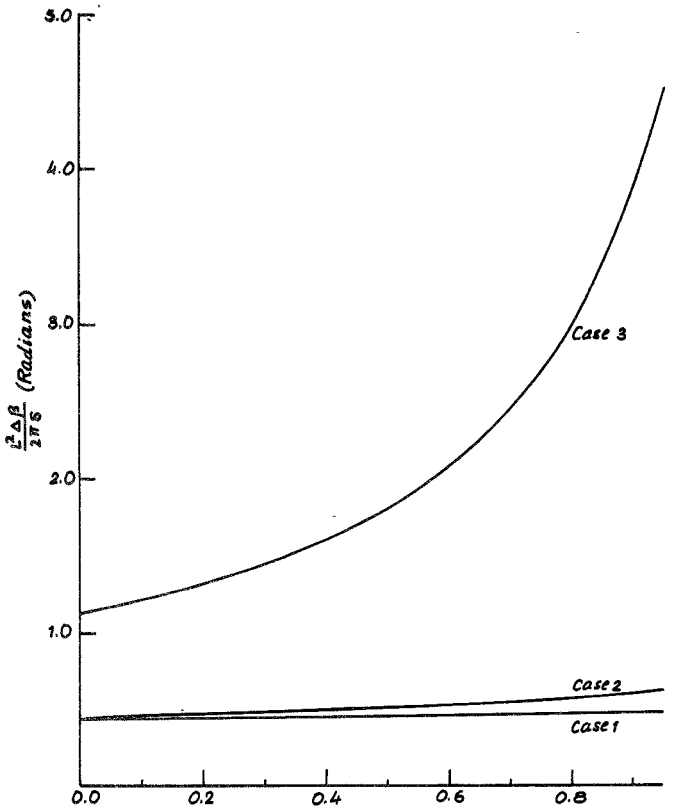

Fig. 2. Normalized differential phase shift versus magnetic field for different configurations. $\omega = 18$ GHz, $4\pi M_0 = 2.8$ kOe, $H_a = 9.0$ kOe (for Zh_2Y [3]).

properties M_0 and H_a. This limits the use of a particular slab in a narrow band of frequencies. Dielectric loading [4] may improve the band performance.

It is noteworthy that (1)–(4) are approximately valid only for very thin slabs. The rigorous derivation of differential phase shift and its applications are currently under investigation. The results will be published later.

References

[1] I. Bady, "Ferrites with planar anisotropy at microwave frequencies," *IRE Trans. Microwave Theory Tech.*, vol. MTT-9, pp. 52–62, Jan. 1961.
[2] B. Lax, K. J. Button, and L. M. Roth, "Ferrite-phase shifters in rectangular waveguides," *J. Appl. Phys.*, vol. 25, p. 1414, 1954.
[3] J. Smit and H. P. J. Wijn, *Ferrites*. Eindhoven, The Netherlands: Philips Tech. Library, 1959, p. 204, table 39.1.
[4] K. J. Button and M. G. Durgin, "Broadband differential phase shifters," Mass. Inst. Technol., Cambridge, Mass. Inst. Technol. Lincoln Lab. Quart. Progr. Rep. Solid State Res., May 1958.

Electric-Field Distribution Along Finite Length Lossy Dielectric Slabs in Waveguide

L. M. LIU, STUDENT MEMBER, IEEE, F. J. ROSENBAUM, SENIOR MEMBER, IEEE, AND W. F. PICKARD, SENIOR MEMBER, IEEE

***Abstract*—A procedure is given to calculate the reflection and transmission coefficients of a full-height dielectric slab centered in a rectangular waveguide. The effects of loss and of finite length are included. The magnitude squared of the electric field along the slab is calculated in order to predict inhomogeneous heat input to the sample. These results are compared with experimental measurements on several materials and the pupae of *Tenebrio molitor*.**

Manuscript received July 24, 1975; revised November 5, 1975. This work was supported in part by the U.S. Public Health Service under Grant HSAA-5504-FR-06115-05.

The authors are with the Department of Electrical Engineering, Washington University, St. Louis, MO 63130.

I. Introduction

The presence of standing waves in biological specimens, caused by internal nonuniformities, or by reflection from the boundaries of the specimen, can lead to localized heating. The distribution of the electromagnetic (EM) fields induced in such tissue has been modeled for planar, cylindrical, and spherical bodies under plane-wave or near-field illumination [1]–[8]. Experiments in which the biological specimen is placed in a waveguide for the purpose of irradiation have also been reported [9]–[11]. Field concentration effects occur in waveguides inhomogeneously loaded with a dielectric medium. If the dielectric is lossy, these effects can produce excess absorption of the microwave energy [12]–[14] in addition to the nonuniform absorption caused by the standing waves.

In this short paper, the biological specimen is modeled as a lossy dielectric slab of finite length inserted along the center line of a waveguide and calculations are presented for the following: 1) the magnitude of the electric field along the slab, 2) transmission and reflection coefficients, and 3) the percentage of incident power absorbed. The techniques and results to be presented here can also be applied to the calculation of power dissipation and heating in waveguide components such as attenuators and phase shifters.

II. Theory

Consider a slab of dielectric material of width D, length l, relative dielectric constant ε_r, and loss tangent $\tan\delta$, located along the center line of a rectangular waveguide of width a as shown in Fig. 1. The slab fills the height b of the waveguide. Assuming that a TE_{10} wave is incident from $-\infty$, the transverse components of the electric and magnetic fields can be expressed as a linear combination of higher order modes [15] in each of the three regions shown in the figure.

In Front of the Slab (Region I): $-\infty < z < 0$

$$E_y = f_1(x)e^{-jh_1 z} + \sum_{n=1,3,5\cdots}^{\infty} a_n f_n(x)e^{jh_n z} \tag{1a}$$

$$H_x = \frac{-f_1(x)}{Z_1} e^{-jh_1 z} + \sum_{n=1,3,5\cdots}^{\infty} \frac{a_n}{Z_n} f_n(x)e^{jh_n z}. \tag{1b}$$

In the Slab (Region II): $0 < z < l$

$$E_y = \sum_{m=1,3,5\cdots}^{\infty} a_m' g_m(x)e^{-\gamma_m z} + \sum_{m=1,3,5\cdots}^{\infty} b_m' g_m(x)e^{\gamma_m z}. \tag{2a}$$

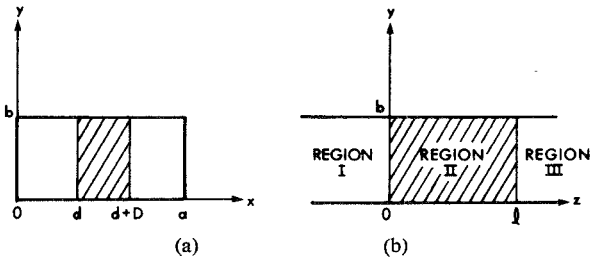

Fig. 1. Configuration of a finite length lossy dielectric slab located in a rectangular waveguide. (a) Cross-sectional view in a yx plane (i.e., down the guide) for which $0 < z < l$. (b) Cross-sectional view in a yz plane for which $d < x < d + D$.

$$H_x = -\sum_{m=1,3,5\cdots}^{\infty} \frac{a_m'}{Z_m'} g_m(x) e^{-\gamma_m z} + \sum_{m=1,3,5\cdots}^{\infty} \frac{b_m'}{Z_m'} g_m(x) e^{\gamma_m z}. \quad (2b)$$

Beyond the Slab (Region III): $l < z < \infty$

$$E_y = \sum_{t=1,3,5\cdots}^{\infty} a_t' f_t(x) e^{-jh_t z} \quad (3a)$$

$$H_x = -\sum_{t=1,3,5\cdots}^{\infty} \frac{a_t'}{Z_t'} f_t(x) e^{-jh_t z}. \quad (3b)$$

Here the quantities a, b are complex-mode amplitudes. The amplitude of the incident field is taken as unity; h_n and γ_m are the longitudinal propagation constants of the empty guide and inhomogeneously loaded guide, respectively. The mode functions are of the form

$$f_n(x) = \sqrt{\frac{2}{a}} \sin \frac{n\pi x}{a} \quad (4)$$

where a is the waveguide width, and

$$g_m(x) = W_m \begin{cases} \dfrac{1}{k_{1m}} \sin k_{1m} x, & 0 < x < d \\ \dfrac{\cos k_{1m} d}{k_{2m} \sin \dfrac{k_{2m} D}{2}} \cos k_{2m}\left(x - \dfrac{a}{2}\right), & d < x < d + D \\ -\dfrac{1}{k_{1m}} \sin k_{1m}(x - a), & d + D < x < a. \end{cases} \quad (5)$$

The normalization factor W_m (see the Appendix) is obtained from

$$\int_0^a g_m(x) g_m^*(x)\, dx = 1. \quad (6)$$

The wave impedances of the empty and the dielectric loaded-guide are given by

$$Z_n = \frac{k_0}{h_n} \sqrt{\frac{\mu_0}{\varepsilon_0}} \quad (7a)$$

and

$$Z_m' = \frac{jk_0}{\gamma_m} \sqrt{\frac{\mu_0}{\varepsilon_0}} \quad (7b)$$

where k_{1m}, k_{2m}, and γ_m satisfy the following equations:

$$k_{2m}^2 - k_{1m}^2 = (\varepsilon_r - 1)k_0^2 - j\varepsilon_r k_0^2 \tan \delta \quad (8)$$

$$k_{1m}^2 = k_0^2 + \gamma_m^2 \quad (9)$$

$$k_{2m}^2 = \varepsilon_r k_0^2 (1 - j \tan \delta) + \gamma_m^2 \quad (10)$$

where $k_0 = \omega/c$; c is the speed of light in vacuum. Also

$$h_n^2 = k_0^2 - \left(\frac{n\pi}{a}\right)^2, \quad \text{for } n = 1,3,5\cdots. \quad (11)$$

III. Field Problem at the Waveguide Discontinuities

At the boundaries $z = 0$, l, E_y, and H_x are continuous. By matching the fields at the boundaries the following system of linear equations results:

At $z = 0$:

$$f_1(x) + \sum_{n=1,3,5\cdots}^{\infty} a_n f_n(x) = \sum_{m=1,3,5\cdots}^{\infty} (a_m + b_m) g_m(x) \quad (12)$$

$$\frac{-f_1(x)}{Z_1} + \sum_{n=1,3,5\cdots}^{\infty} \frac{a_n f_n(x)}{Z_n} = \sum_{m=1,3,5\cdots}^{\infty} \left(-\frac{a_m'}{Z_m'} + \frac{b_m'}{Z_m'}\right) g_m(x) \quad (13)$$

At $z = l$:

$$\sum_{m=1,3,5\cdots}^{\infty} (a_m' e^{-\gamma_m l} + b_m' e^{\gamma_m l}) g_m(x) = \sum_{t=1,3,5\cdots}^{\infty} a_t'' f_t(x) e^{-jh_t l} \quad (14)$$

$$\sum_{m=1,3,5\cdots}^{\infty} \left(-\frac{a_m'}{Z_m'} e^{-\gamma_m l} + \frac{b_m'}{Z_m'} e^{\gamma_m l}\right) g_m(x) = \sum_{t=1,3,5\cdots}^{\infty} -\frac{a_t''}{Z_t} f_t(x) e^{-jh_t l}. \quad (15)$$

Using Chang's procedure [16] and recognizing that the $f_n(x)$ form an orthonormal set, i.e.,

$$\int_0^a f_n(x) f_m(x)\, dx = \delta_{nm} \quad (16)$$

(12) and (13) yield

$$1 + a_1 = \sum_{m=1,3,5\cdots}^{\infty} (a_m' P_{1m} + b_m' P_{1m}) \quad (17)$$

$$-\frac{1}{Z_1} + \frac{a_1}{Z_1} = \sum_{m=1,3,5\cdots}^{\infty} \left(-\frac{a_m'}{Z_m'} + \frac{b_m'}{Z_m'}\right) P_{1m} \quad (18)$$

and

$$a_n = \sum_{m=1,3,5\cdots}^{\infty} (a_m' + b_m') P_{nm}, \quad n \neq 1 \quad (19)$$

$$\frac{a_n}{Z_n} = \sum_{n=1,3,5\cdots}^{\infty} \left(\frac{-a_m'}{Z_m'} + \frac{b_m'}{Z_m'}\right) P_{nm}, \quad n \neq 1 \quad (20)$$

where

$$P_{nm} = \int_0^a f_n(x) g_m(x)\, dx, \quad n = 1,3,5\cdots, \quad m = 1,3,5\cdots. \quad (21)$$

From (17) and (18) a_1 can be eliminated with the result

$$\sum_{m=1,3,5\cdots}^{\infty} \frac{1}{2}\left[\left(1 + \frac{Z_1}{Z_m'}\right) a_m' + \left(1 - \frac{Z_1}{Z_m'}\right) b_m'\right] P_{1m} = 1. \quad (22)$$

In a similar fashion (19) and (20) yield

$$\sum_{m=1,3,5\cdots}^{\infty} \frac{1}{2}\left[\left(1 + \frac{Z_n}{Z_m'}\right) a_m' + \left(1 - \frac{Z_n}{Z_m'}\right) b_m'\right] P_{nm} = 0, \quad n = 3,5\cdots. \quad (23)$$

These may be written as

$$\sum_{m=1,3,5\cdots}^{\infty} \frac{1}{2}\left[\left(1 + \frac{Z_n}{Z_m'}\right) a_m' + \left(1 - \frac{Z_n}{Z_m'}\right) b_m'\right] P_{nm} = \delta_{n1}, \quad n = 1,3,5\cdots. \quad (24)$$

Likewise, from (14) and (15), one obtains

$$\sum_{m=1,3,5\cdots}^{\infty}\left[\left(\frac{1}{Z_n}-\frac{1}{Z_m'}\right)e^{-\gamma_m l}a_m'+\left(\frac{1}{Z_n}+\frac{1}{Z_m'}\right)e^{\gamma_m l}b_m'\right]P_{nm}=0,\qquad n=1,3,5\cdots. \quad (25)$$

Equations (24) and (25) represent two infinite sets of linear equations with two infinite sets of variables which may be solved simultaneously, by numerical means, to find values of the complex a_m', b_m'. The reflection coefficient for the TE_{10} mode in Region I is given by (17). The transmission coefficient, in Region III, is obtained by multiplying both sides of (14) by $f_1(x)$ and integrating over the waveguide width

$$a_1'' = e^{jh_1 l}\sum_{m=1,3,5\cdots}^{\infty}[a_m'e^{-\gamma_m l}+b_m'e^{\gamma_m l}]P_{1m}. \quad (26)$$

The relative heating in the lossy slab depends on

$$|E_y|^2=\sum_{n=1,3,5\cdots}^{\infty}\sum_{m=1,3,5\cdots}^{\infty}[a_m'a_n'^{*}e^{-(\gamma_m+\gamma_n^{*})z}+a_m'b_m'^{*}e^{-(\gamma_m-\gamma_n^{*})z}+b_m'a_n'^{*}e^{(\gamma_m-\gamma_n^{*})z}+b_m'b_n'^{*}e^{(\gamma_m+\gamma_n^{*})z}]g_m(x)g_n^{*}(x). \quad (27)$$

IV. Results

Since the higher order modes generated at the ends of the slab decay rapidly for large n and m, it is reasonable to truncate the infinite system of equations and use an $N \times N$ matrix in the computations of the a_m and b_m. The computation was carried out on a PDP-11 computer using double precision arithmetic. For the numerical results to be presented here only five modes were included since sample calculations showed that the use of $N = 5$ yields the same transmission and reflections coefficients as does the use of six or more modes. Some experimental results for X-band waveguide are summarized in the following along with the predictions of our theoretical analysis.

1) Teflon slab with $l = 25.4$ mm, $D = 5.0$ mm, $\varepsilon_r = 2.04$, $\tan\delta = 0.0$, $a = 22.9$ mm, and $f = 9.0$ GHz. Fig. 2 compares calculated values of $|E_y|^2$ $x = a/2$ with values measured by probing the field along the center line of the slab using a slotted line. The curves were normalized to the same maximum amplitude.

Let $|E_1|^2$, $|E_2|^2$, and $|E_3|^2$ denote, respectively, the squared amplitudes at the first maximum, the minimum, and the second maximum. The comparison of the ratios $|E_1|^2/|E_2|^2$ and $|E_3|^2/|E_2|^2$ between the calculated and measured values is summarized in Table I. Some experimental error results from surface waves launched in the slot by the probe; but, generally, the agreement is good, particularly at the extrema.

2) n—Silicon with $l = 2.22$ mm, $D = 6.7$ mm, $\varepsilon_r = 12$, $\tan\delta = 1.0$. Normalized $|E_y|^2$ $x = a/2$ for the measured and calculated values are plotted in Fig. 3. Note that the field decays rapidly for this lossy sample.

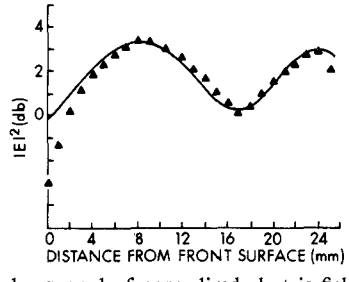

Fig. 2. Magnitude squared of normalized electric field as a function of position along center line of Teflon slab with $D = 5.0$ mm, $l = 25.4$ mm, $\varepsilon_r = 2.04$, and $\tan\delta = 0$, at 9.0 GHz. Calculated (————). Measured (Δ).

TABLE I
Comparison of Standing-Wave Ratio Inside Teflon Slab ($|E_1|^2/|E_2|^2$ and $|E_3|^2/|E_2|^2$)

	Measured	Calculated
$\lvert E_1\rvert^2 / \lvert E_2\rvert^2$	2.09	2.02
$\lvert E_3\rvert^2 / \lvert E_2\rvert^2$	1.95	1.87

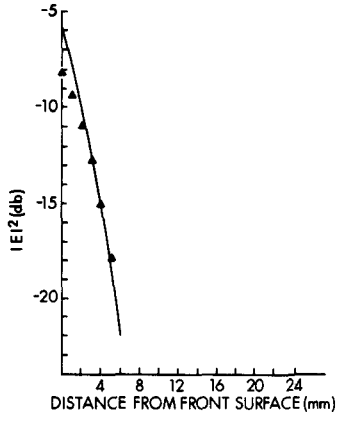

Fig. 3. Magnitude squared of normalized electric field as a function of position along center line of silicon slab with $D = 6.7$ mm, $l = 22.2$ mm, $\varepsilon_r = 12$, and $\tan\delta = 1$, at 9.0 GHz. Calculated (————). Measured (Δ).

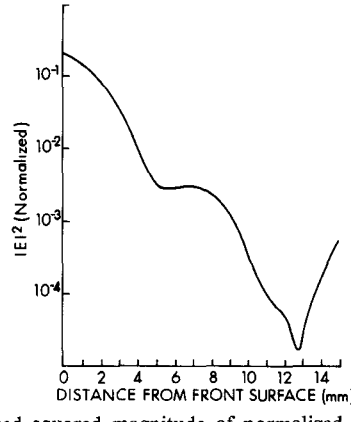

Fig. 4. Calculated squared magnitude of normalized electric field as a function of position along center line of lossy dielectric slab with $D = 5.0$ mm, $l = 15.0$ mm, $\varepsilon_r = 30$, and $\tan\delta = 0.6$, at 9.0 GHz.

3) The width of the slab ($D = 5.0$ mm), its dielectric constant ($\varepsilon_r = 30$), and its loss tangent ($\tan\delta = 0.6$) are chosen to match those reported by Lindauer *et al.* [10] for a *Tenebrio* pupa.

The calculated $|E_y|^2$ $x = a/2$ distribution along the center line of the slab is shown in Fig. 4. Clearly, the maximum heating should occur at the front surface of the slab, and the heat input will be nonuniform along the length of the sample. Standing wave measurements on sample pupae [10] show a maximum field near the center of the pupae.

This difference may be due to the fact that the experimental sample fills only about one-third of the waveguide height: it is possible that the relative maximum near $z = 0.8$ in Fig. 4 increases in the partially filled height case. Calculated reflection and transmission coefficients and the fraction of the incident

TABLE II
REFLECTION AND TRANSMISSION COEFFICIENTS AND ABSORPTION FOR $\varepsilon_r = 30$, $\tan \delta = 0.6$, $D = 5.0$ mm, $l = 15.0$ mm AS A FUNCTION OF FREQUENCY

Frequency (GHz)	Reflection Coefficient	Transmission Coefficient	Fraction Absorbed
8	0.844 /-172.6°	0.0058 /1.08°	0.288
9	0.778 /-173.4°	0.0044 /-153.4°	0.395
10	0.727 /-168.3°	0.0079 /-27.9°	0.471
11	0.617 /-176.1°	0.0096 /157.42°	0.619
12	0.544 /-175.9°	0.0118 /-169.3°	0.704

TABLE III
REFLECTION AND TRANSMISSION COEFFICIENTS AND ABSORPTION FOR THE SLAB OF TABLE II AT 9.0 GHz AND A VARIETY OF DIELECTRIC CONSTANTS

ε_r	Reflection Coefficient	Transmission Coefficient	Fraction Absorbed
21	0.794 /-168.4°	0.0126 /-82.7°	0.369
30	0.778 /-173.4°	0.0045 /-153.4°	0.395
51	0.801 /179.8°	0.0026 /130.36°	0.358

power absorbed for this lossy slab are given in Table II for several frequencies and in Table III for several different dielectric constants at 9 GHz. The fraction of incident power absorbed is more sensitive to frequency than to relative dielectric constant. The absorption at 9.0 GHz and $\varepsilon_r = 30$ (39.4 percent) compares favorably with that observed in real pupae (32 percent) [10].

V. Discussion

The agreement between theory and experiment which is displayed in Figs. 2 and 3 and in Table I leads us to believe that the five-term field approximation technique will be adequate for a variety of applications.

For the cases examined here, maximum heating always occurred at the front surface of the slab and no significant secondary maxima were observed. We believe, however, that other combinations of slab parameters could well result in significant standing waves along the slab and a resultant inhomogeneity of heat input.

The effect of partial filling in the height of the guide was not examined due to its complexity and due to the agreement between the power absorption calculated for a full-height slab and that observed for actual pupae. We note, however, that the calculated and observed field distributions for this configuration do differ significantly and caution therefore against the uncritical application of these techniques to partial-height obstacles.

Appendix

The normalization factor W_m for function $g_m(x)$ in (5) is given by

$$W_m = \left[\frac{1}{|k_{1m}|^2} \left\{ \frac{\sin (k_{1m} - k_{1m}^*)d}{k_{1m} - k_{1m}^*} \quad \frac{\sin (k_{1m} + k_{1m}^*)d}{k_{1m} + k_{1m}^*} \right\} + \frac{|\cos k_{1m} d|^2}{\left| k_{2m} \sin \frac{k_{2m} D}{2} \right|^2} \cdot \left\{ \frac{\sin (k_{2m} - k_{2m}^*) \frac{D}{2}}{k_{1m} - k_{1m}^*} + \frac{\sin (k_{2m} + k_{2m}^*) \frac{D}{2}}{k_{2m} + k_{2m}^*} \right\} \right]^{-1/2}. \quad \text{(A1)}$$

References

[1] A. R. Shapiro, R. F. Lutomirski, and H. T. Yura, "Induced fields and heating within a cranial structure irradiated by an electromagnetic plane wave," *IEEE Microwave Theory Tech. (Special Issue on Biological Effects of Microwaves)*, vol. MTT-19, pp. 187–197, Feb. 1971.

[2] A. W. Guy, "Analyses of electromagnetic fields induced in biological tissues by thermographic studies on equivalent phantom models," *IEEE Trans. Microwave Theory Tech. (Special Issue on Biological Effects of Microwaves)*, vol. MTT-19, pp. 205–214, Feb. 1971.

[3] ——, "Electromagnetic fields and relative heating patterns due to a rectangular aperture source in direct contact with bilayered biological tissue," *IEEE Microwave Theory Tech. (Special Issue on Biological Effects of Microwaves)*, vol. MTT-19, pp. 214–223, Feb. 1971.

[4] H. S. Ho, A. W. Guy, R. S. Spigelmann, and J. F. Lehmann, "Microwave heating of simulated human limbs by aperture sources," *IEEE Trans. Microwave Theory Tech. (Special Issue on Biological Effects of Microwaves)*, vol. MTT-19, pp. 224–231, Feb. 1971.

[5] H. N. Kritikos and H. P. Schwan, "Hot spots generated in conducting spheres by electromagnetic waves and biological implications," *IEEE Trans. Biomed. Eng.*, vol. BME-19, pp. 53–58, Jan. 1972.

[6] J. C. Lin, A. W. Guy, and C. C. Johnson, "Power deposition in a spherical model of man exposed to 1–20-MHz electromagnetic fields," *IEEE Trans. Microwave Theory Tech. (1973 Symposium Issue)*, vol. MTT-21, pp. 791–797, Dec. 1973.

[7] W. T. Joines and R. J. Spiegel, "Resonance absorption of microwaves by the human skull," *IEEE Trans. Biomed. Eng.*, vol. BME-21, pp. 46–48, Jan. 1974.

[8] D. E. Livesay and K. M. Chen, "Electromagnetic fields induced inside arbitrarily shaped biological bodies," *IEEE Trans. Microwave Theory Tech.*, vol. MTT-22, pp. 1273–1280, Dec. 1974.

[9] R. L. Carpenter and E. M. Livstone, "Evidence for nonthermal effects of microwave radiation: Abnormal development of irradiated insect pupae," *IEEE Trans. Microwave Theory Tech.*, vol. MTT-19, pp. 173–178, Feb. 1971.

[10] G. A. Lindauer, L. M. Liu, G. W. Skewes, and F. J. Rosenbaum, "Further experiments seeking evidence of nonthermal effects of microwave radiation," *IEEE Trans. Microwave Theory Tech.*, vol. MTT-22, pp. 790–793, Aug. 1974.

[11] L. M. Liu, F. J Rosenbaum, and W. F. Pickard, "The relation of teratogenesis in *Tenebrio molitor* to the incidence of low-level microwaves," *IEEE Trans. Microwave Theory Tech.* (Short Papers), vol. MTT-23, pp. 929–931, Nov. 1975.

[12] R. M. Arnold and F. J. Rosenbaum, "Nonreciprocal wave propagation in semiconductor loaded waveguides in the presence of a transverse magnetic field," *IEEE Trans. Microwave Theory Tech.*, vol. MTT-19, pp. 57–65, Jan. 1971.

[13] V. R. Bui and R. R. J. Gagné, "Dielectric losses in an *H*-plane-loaded rectangular waveguide," *IEEE Trans. Microwave Theory Tech.* (Short Papers), vol. MTT-20, pp. 621–623, Sept. 1972.

[14] F. E. Gardiol and O. Parriaux, "Excess losses in *H*-plane-loaded waveguides," *IEEE Trans. Microwave Theory Tech.*, vol. MTT-21, pp. 457–461, July 1973.

[15] R. E. Collin, *Field Theory of Guided Waves* (International Pure and Applied Physics Ser.). New York: McGraw-Hill, 1966.

[16] C. T. M. Chang, "Equivalent circuit for partially dielectric-filled rectangular waveguide junctions," *IEEE Trans. Microwave Theory Tech.*, vol. MTT-21, pp. 403–411, June 1973.

Scattering of Microwaves by Dielectric Materials Used in Laboratory Animal Restrainers

JAMES C. LIN AND CHUAN-LIN WU, STUDENT MEMBER, IEEE

***Abstract*—In most experimental investigations of the biological effects of microwave radiation, it is necessary to use low-loss dielectric materials for restraining animals under irradiation. Because of the complexity of the analysis of the animal–restrainer combination, an analysis is made of the scattering of microwave fields by a simplified model of the restrainer with no animal present. The model chosen is that of a plane wave incident at an arbitrary angle upon a rectangular slab of finite width and thickness. Numerical results indicate that the scattered fields within a square region of one wavelength in distance from the slab surfaces are greatly enhanced and highly nonuniform. In particular, the maxima for parallel incidence exceed those for normal incidence by almost a factor of 2.**

Manuscript received December 30, 1974; revised November 3, 1975. This work was supported in part by the Office of Naval Research under Contract N00014-75-C-0637, and in part by National Science Foundation Grant ENG 75-15227.

The authors are with the Department of Electrical Engineering, Wayne State University, Detroit, MI 48202.